

## Stress intensity factors for periodic edge cracks in a semi-infinite medium with distributed eigenstrain

A. M. Afsar† and S. R. Ahmed‡

*Mechanical Engineering Department, Bangladesh University of Engineering and Technology,  
Dhaka 1000, Bangladesh*

*(Received November 10, 2004, Accepted June 8, 2005)*

**Abstract.** This study analyzes stress intensity factors for a number of periodic edge cracks in a semi-infinite medium subjected to a far field uniform applied load along with a distribution of eigenstrain. The eigenstrain is considered to be distributed arbitrarily over a region of finite depth extending from the free surface. The cracks are represented by a continuous distribution of edge dislocations. Using the complex potential functions of the edge dislocations, a simple as well as effective method is developed to calculate the stress intensity factor for the edge cracks. The method is employed to obtain the numerical results of the stress intensity factor for different distributions of eigenstrain. Moreover, the effect of crack spacing and the intensity of the normalized eigenstress on the stress intensity factor are investigated in details. The results of the present study reveal that the stress intensity factor of the periodic edge cracks is significantly influenced by the magnitude as well as distribution of the eigenstrain within the finite depth. The eigenstrains that induce compressive stresses at and near the free surface of the semi-infinite medium reduce the stress intensity factor that, in turn, contributes to the toughening of the material.

**Key words:** stress intensity factor; eigenstrain; edge dislocation; periodic edge cracks; semi-infinite medium.

---

### 1. Introduction

Eigenstrain (Mura 1987) is the generic name of such non-elastic strains as thermal expansion, phase transformation, initial strains, plastic strains, and mismatch strains. The incompatibility of these eigenstrains results in eigenstresses that are self-equilibrated internal stresses, conventionally known as residual stresses. The free surface of a semi-infinite medium may undergo various kinds of processes like cutting, grinding, milling, etc. as well as shot-peening and heat treatment processes. Consequently, eigenstrain is developed at and near the free surface of the medium. Again, the free surface may be exposed to temperatures different from that in other part of the medium, which results in nonuniform temperature distribution near the free surface. This also causes the eigenstrain to develop at and near the free surface. In order to understand and improve the fracture characteristics of the medium, an accurate and reliable analysis of the effect of this eigenstrain on the stress intensity factor is of great practical importance.

---

† Assistant Professor, Corresponding author, E-mail: [mdafsarali@me.buet.ac.bd](mailto:mdafsarali@me.buet.ac.bd)

‡ Associate Professor

So far, stress intensity factors of edge cracks in semi-infinite media have been studied extensively for various loading conditions, such as, far field uniform load, uniform pressure over part of the crack surface, point load, etc. The works of Stallibrass (1970), Hartranft and Sih (1973), Sneddon and Das (1971), Sneddon (1946), and Afsar (1997) may be cited as a few examples. More recently, Sekine and Afsar (1999) considered a single edge crack in a semi-infinite functionally graded material (FGM) and investigated the effect of eigenstrain on the stress intensity factor followed by the optimization of composition profile for desired brittle fracture characteristics in the FGM medium. As an extension of their work, they carried out further researches to compute the material distribution in a thick-walled FGM pipe (Afsar and Sekine 2001) and an FGM coating around a circular hole in an infinite medium (Afsar and Sekine 2002) with an edge crack emanating from the inner surfaces of the cylinder and hole, respectively.

In this study, we concentrate on the periodic edge cracks in a semi-infinite medium of homogeneous material with distributed eigenstrain. It is recognized that eigenstrain is inherently developed in an FGM body due to nonuniform coefficient of thermal expansion, as a result of cooling from sintering temperature. However, it may also be developed in a semi-infinite medium of homogeneous material due to various machining and heat treatment processes. This eigenstrain is considered here for investigating its effects on the stress intensity factor for periodic edge cracks in the semi-infinite medium of homogeneous material. In our present analysis, the eigenstrain is assumed to be distributed over a region of finite depth that extends from the free surface. This assumption is fairly reasonable as the various machining and heat treatment processes affect the region whose depth from the free surface is indeed small. For such a problem, a simple as well as effective method is developed to evaluate the stress intensity factors by using the method of complex potential functions of edge dislocations representing the cracks. To demonstrate the method, some numerical results are obtained and presented for different functional forms of eigenstrain distribution. Furthermore, the effects of crack spacing and the intensity of the normalized eigenstress on the stress intensity factor are investigated in details.

## 2. Model of the problem

Shown in Fig. 1 is a semi-infinite medium, which is subjected to a far-field uniform applied stress  $\sigma_x^0$ . The region of finite depth  $w$  has an arbitrary distribution of eigenstrain  $\varepsilon^*$ , which is a function of  $y$  only. Shown in the figure are also a number of periodic edge cracks of equal length, all of which are perpendicular to the free surface. The length of the cracks and the distance between them are denoted by  $a$  and  $d$ , respectively. A principal coordinate system  $x$ - $y$  is considered, the origin of which is located at the mouth of the central crack. Further, a secondary coordinate system  $x_m$ - $y_m$  is considered, the origin of which is located at the mouth of the crack other than the central one, where  $m = \pm 1, \pm 2, \pm 3, \dots, \pm N$ . If we define two complex variables  $z = x + iy$  and  $z_m = x_m + iy_m$  that represent the coordinate of a point with reference to the principal and secondary coordinate systems, respectively, the following relationship holds between them

$$z_m = z - md \quad (1)$$

For the model outlined above, a method is developed to evaluate the stress intensity factor for plane stress in order to investigate the effect of eigenstrain on the stress intensity factors.

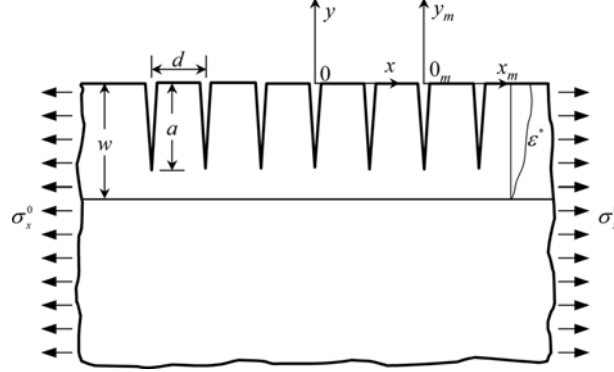


Fig. 1 Analytical model of the problem

### 3. Stress intensity factor

#### 3.1 Stress field in uncracked medium

First, we consider the semi-infinite medium without any cracks. The uncracked semi-infinite medium is subjected to a uniform load  $\sigma_x^0$  along with an arbitrary distribution of eigenstrain  $\varepsilon^*(y)$  in the region of finite depth  $w$ . The resultant stress field in the uncracked semi-infinite medium can be determined by superposition of the stress due to the eigenstrain  $\varepsilon^*(y)$  and the applied load  $\sigma_x^0$ .

The stress due to eigenstrain  $\varepsilon^*(y)$  can be determined following the philosophy outlined by Sekine and Afsar (1999). Since the depth  $w$  is very small compared to that of the lower region of the semi-infinite medium, the eigenstrain  $\varepsilon^*(y)$  in the region of finite depth  $w$  is completely suppressed by the restraining effect from the lower region of the semi-infinite medium. Therefore, the stress developed in the region of finite depth  $w$  due to the eigenstrain can be given by

$$\sigma_x^* = -E \varepsilon^* \quad (2)$$

where  $E$  is the Young's modulus. The stress in the remaining part of the semi-infinite medium due to the eigenstrain is negligible as the region beyond the finite depth  $w$  is of infinite dimension over which the stress is distributed. Thus, the resultant stress field in the region of finite depth  $w$  is  $(\sigma_x^* + \sigma_x^0)$  while the stress beyond  $w$  is approximately equal to the applied stress  $\sigma_x^0$ .

#### 3.2 Cracked semi-infinite medium

The resultant stress field calculated for the uncracked semi-infinite medium in the foregoing is disturbed due to the presence of the cracks. Therefore, it is necessary to determine the redistribution of the stress field in the presence of the cracks. This redistributed stress field is computed by representing the cracks by a continuous distribution of edge dislocations of density  $b_x(s)$  as shown in Fig. 2. First, we consider the central crack. Following the representation of the crack as shown in Fig. 2, the complex potential functions for the edge dislocations can be written as (Afsar 1997)

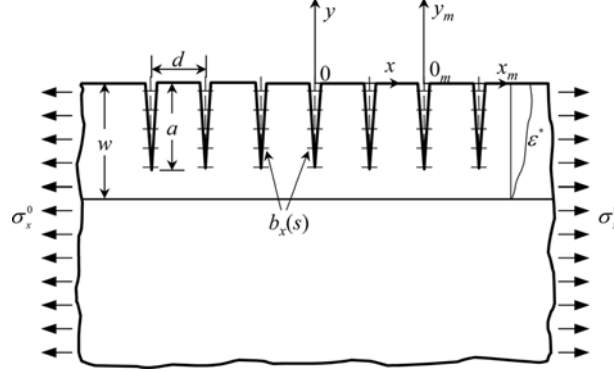


Fig. 2 Representation of cracks by continuous distribution of edge dislocations of density  $b_x(s)$  ( $0 \geq s \geq -a$ )

$$\begin{aligned} \Phi_0(z) = & -\frac{i\mu}{\pi(\kappa+1)} \int_0^a \left[ \frac{1}{z+is} - \frac{1}{z-is} - \frac{2is}{(z-is)^2} \right] b_x(s) ds \\ & + \frac{\mu}{\pi(\kappa+1)} \int_0^a \left[ \frac{1}{z+is} - \frac{1}{z-is} + \frac{2is}{(z-is)^2} \right] b_y(s) ds \end{aligned} \quad (3a)$$

$$\begin{aligned} \Psi_0(z) = & \frac{i\mu}{\pi(\kappa+1)} \int_0^a \left[ \frac{1}{z+is} - \frac{1}{z-is} - \frac{is}{(z+is)^2} + \frac{3is}{(z-is)^2} - \frac{4s^2}{(z-is)^3} \right] b_x(s) ds \\ & + \frac{\mu}{\pi(\kappa+1)} \int_0^a \left[ \frac{1}{z+is} - \frac{1}{z-is} + \frac{is}{(z+is)^2} + \frac{is}{(z-is)^2} - \frac{4s^2}{(z-is)^3} \right] b_y(s) ds \end{aligned} \quad (3b)$$

where

$\mu$  = Shear modulus of rigidity

$b_x(s), b_y(s)$  = Components of dislocation density function

$\kappa$  = Kolosov's constant

=  $3 - 4\nu$  for plane strain

=  $(3 - \nu)/(1 + \nu)$  for plane stress.

The stresses inside an isotropic elastic medium can be expressed in terms of the complex potential functions  $\Phi_0(z)$  and  $\Psi_0(z)$  and their complex conjugates as follows (Muskhelishvili 1975):

$$\sigma_{xx}^0 + \sigma_{yy}^0 = 2[\Phi_0(z) + \overline{\Phi_0(z)}] \quad (4a)$$

$$\sigma_{xx}^0 - \sigma_{yy}^0 + 2i\sigma_{xy}^0 = -2[z\overline{\Phi_0'(z)} + \overline{\Psi_0(z)}] \quad (4b)$$

where the prime represents differentiation with respect to  $z$  and the over bar represents the complex conjugate.

Similarly, the stresses for the dislocations representing the  $m$ th crack can be given by

$$\sigma_{xx}^m + \sigma_{yy}^m = 2[\Phi_m(z_m) + \overline{\Phi_m(z_m)}] \quad (5a)$$

$$\sigma_{xx}^m - \sigma_{yy}^m + 2i\sigma_{xy}^m = -2[z_m\overline{\Phi_m'(z_m)} + \overline{\Psi_m(z_m)}] \quad (5b)$$

where  $\Phi_m(z_m)$  and  $\Psi_m(z_m)$  are the complex potential functions for edge dislocations representing the  $m$ th crack. These functions have the same expressions as those of Eq. (3), except that  $z$  is replaced by  $z_m$ . Finally, the resultant stresses due to the edge dislocations representing all the cracks are obtained by the method of superposition as follows:

$$\sigma_{xx} = \sigma_{xx}^0 + \sum_{m=-N}^N \sigma_{xx}^m ; N \neq 0 \quad (6a)$$

$$\sigma_{yy} = \sigma_{yy}^0 + \sum_{m=-N}^N \sigma_{yy}^m ; N \neq 0 \quad (6b)$$

$$\sigma_{xy} = \sigma_{xy}^0 + \sum_{m=-N}^N \sigma_{xy}^m ; N \neq 0 \quad (6c)$$

Now, the redistributed stress field in the cracked medium can be determined by adding the stress components in Eqs. (6) to the stress computed for the uncracked semi-infinite medium. The redistributed stress field must satisfy the boundary conditions along the traction free crack surfaces, i.e.,

$$\sigma_{xx}^0 + \sum_{m=-N}^N \sigma_{xx}^m + \sigma_x^* + \sigma_x^0 = 0 ; x = 0, 0 \geq y \geq -a \quad (7a)$$

$$\sigma_{xy}^0 + \sum_{m=-N}^N \sigma_{xy}^m = 0 ; x = 0, 0 \geq y \geq -a \quad (7b)$$

The above boundary conditions are written for the central crack.

Now, using Eqs. (1), (4)-(5), boundary conditions of Eq. (7), potential functions for the edge dislocations representing the central and the  $m$ th cracks, and replacing  $y$  by  $-y$ , we obtain

$$\frac{2\mu}{\pi(\kappa+1)} \left[ \int_0^a \frac{b_x(s)}{y-s} ds + \int_0^a \hat{k}(y,s) b_x(s) ds + \int_0^a \hat{k}_1(y,s) b_x(s) ds \right] = -(\sigma_x^* + \sigma_x^0) ; 0 \leq y \leq a \quad (8a)$$

$$\frac{2\mu}{\pi(\kappa+1)} \left[ \int_0^a \frac{b_y(s)}{y-s} ds + \int_0^a \hat{k}(y,s) b_y(s) ds - \int_0^a \hat{k}_2(y,s) b_y(s) ds \right] = 0 ; 0 \leq y \leq a \quad (8b)$$

where

$$\hat{k}(y,s) = -\frac{1}{y+s} - \frac{2s}{(y+s)^2} + \frac{4s^2}{(y+s)^3} \quad (9a)$$

$$\begin{aligned} \hat{k}_1(y,s) &= \sum_{m=1}^N \left[ \frac{3(y-s)}{[(y-s)^2 + (md)^2]} - \frac{3(y+s)}{(y+s)^2 + (md)^2} \right] \\ &+ \frac{(y+s)^3 - 3(md)^2(y+s)}{[(y+s)^2 + (md)^2]^2} + \frac{3(md)^2(y-s) - (y-s)^3}{[(y-s)^2 + (md)^2]^2} \end{aligned}$$

$$\left. \frac{4s[(y+s)^3(y-s) - 6(md)^2y(y+s) + (md)^4]}{[(y+s)^2 + (md)^2]^3} \right] \quad (9b)$$

$$\begin{aligned} \hat{k}_2(y, s) = & \sum_{m=1}^N \left[ \frac{y-s}{(y-s)^2 + (md)^2} - \frac{y+s}{(y+s)^2 + (md)^2} \right. \\ & \frac{(y+s)^3 - 3(md)^2(y+s)}{[(y+s)^2 + (md)^2]^2} + \frac{(y-s)^3 - 3(md)^2(y-s)}{[(y-s)^2 + (md)^2]^2} \\ & \left. \frac{4s[(y+s)^3(y-s) - 6y(md)^2(y+s) + (md)^4]}{[(y+s)^2 + (md)^2]^3} \right] \quad (9c) \end{aligned}$$

Eqs. (8a) and (8b) are two singular integral equations and it is seen that there is no coupling between the burgers vectors  $b_x$  and  $b_y$  which give the Mode I and Mode II stress intensity factors, respectively. Since the right side of Eq. (8b) is zero, the burgers vector  $b_y$  induces no stress intensity, i.e., the Mode II stress intensity factor is zero and hence only Eq. (8a) is treated in the sequel.

#### 4. Numerical method of solution

Analytical solution of the singular integral equation as given by Eq. (8a) is not possible. Therefore, a numerical method is adopted to solve the equation. First the singular integral equation is normalized over the interval  $[-1, +1]$  by using the substitutions

$$t = \frac{2s}{a} - 1 \quad (10a)$$

$$\xi = \frac{2y}{a} - 1 \quad (10b)$$

$$P = \frac{D}{(a/w)}, \quad D = \frac{2d}{w} \quad (10c)$$

as

$$\frac{2\mu}{\pi(\kappa+1)} \left[ \int_{-1}^1 \frac{B_x(t)}{(\xi-t)} dt + \int_{-1}^1 k(\xi, t) B_x(t) dt + \int_{-1}^1 k_1(\xi, t) B_x(t) dt \right] = -[\sigma_x^*(\xi) + \sigma_x^0(\xi)]; \quad -1 \leq \xi \leq 1 \quad (11)$$

where

$$k(\xi, t) = -\frac{1}{t + \xi + 2} - \frac{2(t+1)}{(t + \xi + 2)^2} + \frac{4(t+1)^2}{(t + \xi + 2)^3} \quad (12a)$$

$$k_1(\xi, t) = \sum_{m=1}^N \left[ \frac{3(\xi-t)}{[(\xi-t)^2 + (mP)^2]} - \frac{3(\xi+t+2)}{[(\xi+t+2)^2 + (mP)^2]} \right]$$

$$\begin{aligned}
& + \frac{(\xi + t + 2)^3 - 3(mP)^2(\xi + t + 2)}{[(\xi + t + 2)^2 + (mP)^2]^2} + \frac{3(mP)^2(\xi - t) - (\xi - t)^3}{[(\xi - t)^2 + (mP)^2]^2} \\
& - \frac{4(t + 1)[(\xi + t + 2)^3(\xi - t) - 6(mP)^2(\xi + 1)(\xi + t + 2) + (mP)^4]}{[(\xi + t + 2)^2 + (mP)^2]^3} \Big] \quad (12b)
\end{aligned}$$

$$B_x(t) = b_x(s) \quad (12c)$$

The dislocation density function  $B_x(t)$  can be expressed as the product of a fundamental function  $W(t)$ , which characterizes the bounded-singular behavior of  $B_x(t)$ , and a bounded continuous function  $\varphi_x(t)$  in the closed interval  $[-1, +1]$ . Thus

$$B_x(t) = W(t)\varphi_x(t) \quad (13a)$$

In the present case, the fundamental function  $W(t)$  is given by

$$W(t) = \sqrt{\frac{1+t}{1-t}} \quad (13b)$$

Using the Gauss-Jacobi integral formula in the manner similar to that developed by Erdogan *et al.* (1973), the singular integral equation can be converted to a system of linear algebraic equations to determine the unknown  $\varphi_x(t)$  as

$$\begin{aligned}
& \frac{2\mu}{(\kappa + 1)} \left[ \sum_{q=1}^n \varphi_x(t_q)(1 + t_q) \left\{ \frac{1}{\xi_r - t_q} + k(\xi_r, t_q) + k_1(\xi_r, t_q) \right\} \right] \\
& = -\frac{2n+1}{2} [\sigma_x^*(\xi_r) + \sigma^0(\xi_r)]; \quad r = 1, 2, 3, \dots, n \quad (14)
\end{aligned}$$

where the integration and collocation points are, respectively, given by (Hills *et al.* 1996)

$$t_q = \cos\left(\frac{2q-1}{2n+1}\pi\right), \quad q = 1, 2, 3, \dots, n \quad (15a)$$

$$\xi_r = \cos\left(\frac{2r\pi}{2n+1}\right), \quad r = 1, 2, 3, \dots, n \quad (15b)$$

It can be readily shown that the Mode I stress intensity factors can be derived as (Hills *et al.* 1996)

$$K_I = \sqrt{\pi a} \frac{2\mu}{(\kappa + 1)} \sqrt{2} \varphi_x(+1) \quad (16)$$

The solution of Eq. (14) provides the values of  $\varphi_x$  only at the integration points  $t_q$ . The calculation of stress intensity factors, as seen from Eq. (16), requires the value of this function at the crack tip, i.e.,  $\varphi_x(+1)$ . This value can be obtained by the following Krenk's (1975) interpolation formula:

$$\varphi_x(+1) = \frac{2}{2n+1} \sum_{i=1}^n \frac{\sin\left(\frac{2i-1}{2n+1}n\pi\right)}{\tan\left(\frac{2i-1}{2n+1}\frac{\pi}{2}\right)} \varphi_x(t_i) \quad (17)$$

Using Eqs. (14) through (17), stress intensity factors can be calculated for a given applied load and eigenstrain distribution.

## 5. Numerical results and discussion

In this section, some numerical results of stress intensity factors are calculated and presented for various distributions of eigenstrain in the region of finite depth  $w$  of the semi-infinite medium.

The distributions of eigenstrain considered are parabolic 1 distribution:  $\varepsilon^* = \varepsilon^0 \left(1 + \frac{y}{w}\right)^{\frac{1}{2}}$ , parabolic 2 distribution:  $\varepsilon^* = \varepsilon^0 \left(1 - \frac{y^2}{w^2}\right)$ , parabolic 3 distribution:  $\varepsilon^* = \varepsilon^0 \left(1 + \frac{y}{w}\right)^2$ , linear distribution:  $\varepsilon^* = \varepsilon^0 \left(1 + \frac{y}{w}\right)$ , and uniform distribution:  $\varepsilon^* = \varepsilon^0$ . These distributions of eigenstrain are shown in Fig. 3.

Here, it is worthy to mention that although any arbitrary distribution of eigenstrain can be treated, the above five distributions have been chosen merely as few examples. The uniform distribution of eigenstrain, shown in Fig. 3, may occur in the coating of a homogeneous material on another homogeneous substrate as a form of a misfit thermal strain. On the other hand, the non-uniform distributions considered in Fig. 3 might be encountered in the case of functionally graded material (FGM) coatings on a substrate of homogeneous material after cooling from sintering temperature. In

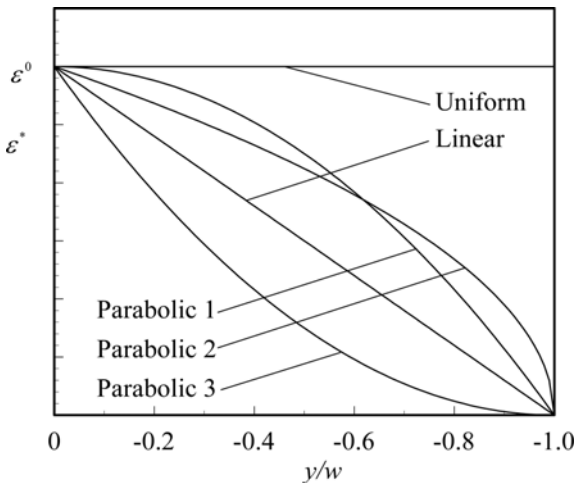


Fig. 3 Distribution of eigenstrains in the region of finite depth  $w$

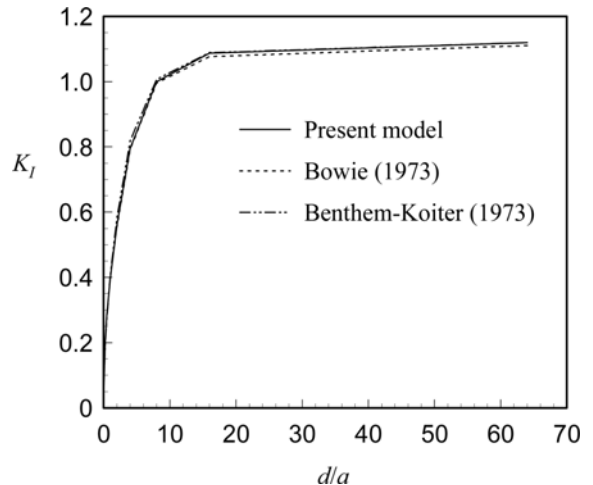


Fig. 4 Comparison of stress intensity factors for a number of periodic edge cracks in a semi-infinite medium under uniform tension

the numerical calculation, the number of collocation and integration points  $n$  is taken as 100, for which the values of the stress intensity factors, calculated by setting  $\varepsilon^* = 0$ , agree well with those obtained by Bowie (1973) and Benthem and Koiter (1973) as shown in Fig. 4. When  $\varepsilon^* = 0$ , the problem reduces to the semi-infinite medium subjected to applied load only.

Fig. 5(a) exhibits the stress intensity factors as a function of normalized crack length  $a/w$  and normalized crack spacing  $d/w$ . The stress intensity factors are normalized dividing them by the true value of the stress intensity factor  $K_e = 1.12152$  for a single edge crack in a semi-infinite medium under a far field uniform load  $\sigma_x^0$  only. The results of Fig. 5(a) correspond to the parabolic 1 distribution of eigenstrain as shown in Fig. 3. In calculating the stress intensity factor, we define a

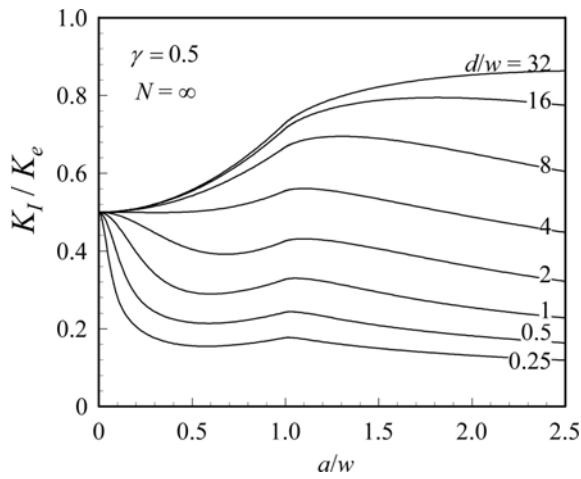


Fig. 5(a) Normalized stress intensity factors for the 'Parabolic 1' distribution of eigenstrain

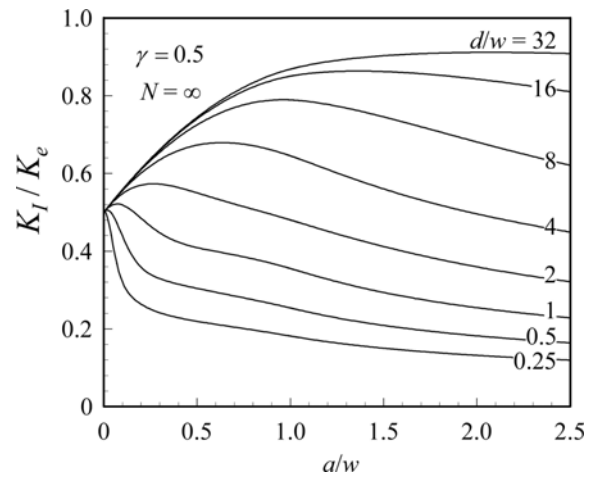


Fig. 5(b) Normalized stress intensity factors for the 'Parabolic 2' distribution of eigenstrain

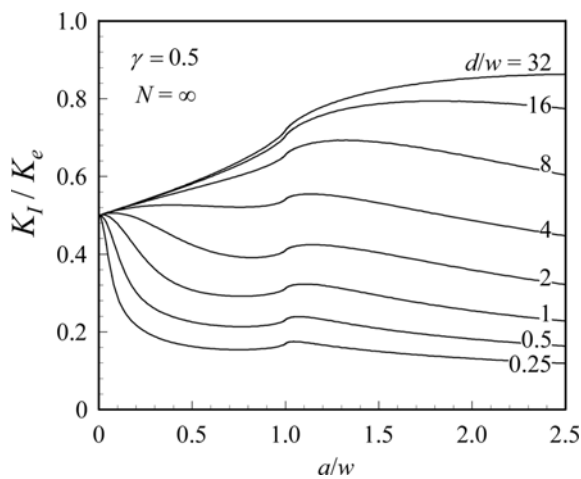


Fig. 5(c) Normalized stress intensity factors for the 'Parabolic 3' distribution of eigenstrain

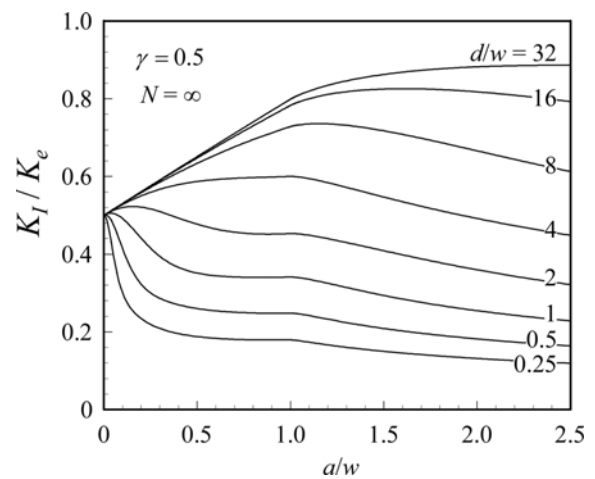


Fig. 5(d) Normalized stress intensity factors for the 'Linear' distribution of eigenstrain

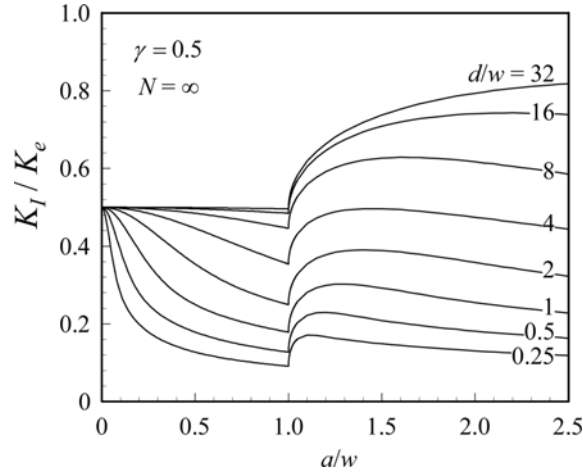


Fig. 5(e) Normalized stress intensity factors for the 'Uniform' distribution of eigenstrain

parameter  $\gamma = E \varepsilon^0 / \sigma_x^0$  in which  $\varepsilon^0$  is the eigenstrain at  $y = 0$  and  $E$  is the Young's modulus of the material. The parameter  $\gamma$ , in fact, is the ratio of eigenstress at  $y = 0$  to the applied stress  $\sigma_x^0$ . The stress intensity factors shown in Fig. 5(a) are obtained for  $\gamma = 0.5$  and infinite number of periodic edge cracks, i.e.,  $N = \infty$ . The eigenstrain is distributed over the region of finite depth  $w$ . Therefore, the crack tip crosses the region of eigenstrain when  $a/w \geq 1$  showing points of inflection on the curves of the stress intensity factor. Figs. 5(b) through 5(e) depict the normalized stress intensity factors for parabolic 2, parabolic 3, linear, and uniform distributions of the eigenstrain, respectively. The curves of all the figures have the same characteristics except that the stress intensity factors for the uniform distribution of eigenstrain have quite sharp points of inflection at  $a/w = 1$ . Further, Figs. 5(a) through 5(e) show, for a fixed value of  $a/w$ , that the stress intensity factor increases with the increase of the crack spacing  $d/w$ . Increasing value of  $d/w$  implies that the cracks are getting

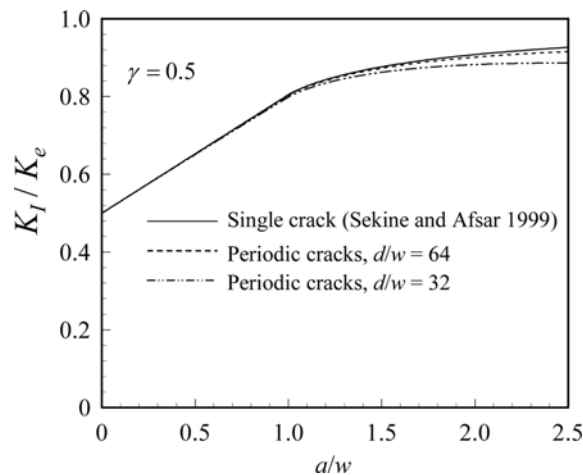


Fig. 6 Comparison of results predicted by the formulations of a single edge crack and periodic edge cracks

apart from each other, i.e., one crack becomes unaffected by the other and a single crack phenomenon is attained. This can be better explained from Fig. 6, which shows the results of the stress intensity factor predicted by the formulations of a single edge crack (Sekine and Afsar 1999) along with those predicted by the present study. The results correspond to the linear distribution of eigenstrain, as shown in Fig. 3, and  $\gamma = 0.5$ . It is observed that the curve of the stress intensity factor for infinite number of periodic edge cracks approaches towards that for the single edge crack as  $d/w$  increases. Thus, it is verified that the present method of calculating stress intensity factors can be applied to the single edge crack problem by setting a large value of  $d/w$ .

Fig. 7(a) illustrates the effect of the distribution of eigenstrain on the stress intensity factors. The results of the stress intensity factor are plotted for the five different distributions of eigenstrain as

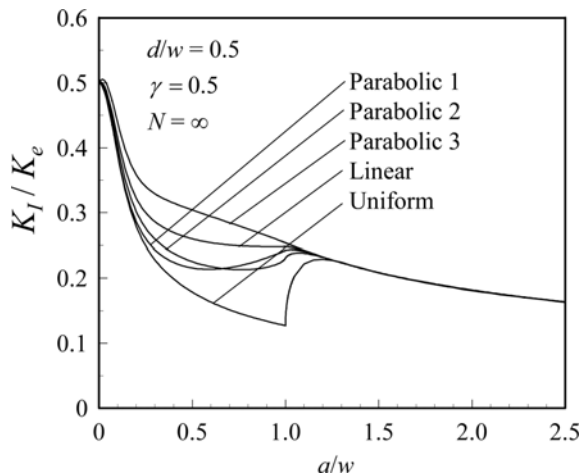


Fig. 7(a) Effect of eigenstrain distribution on the stress intensity factors ( $d/w = 0.5$ )

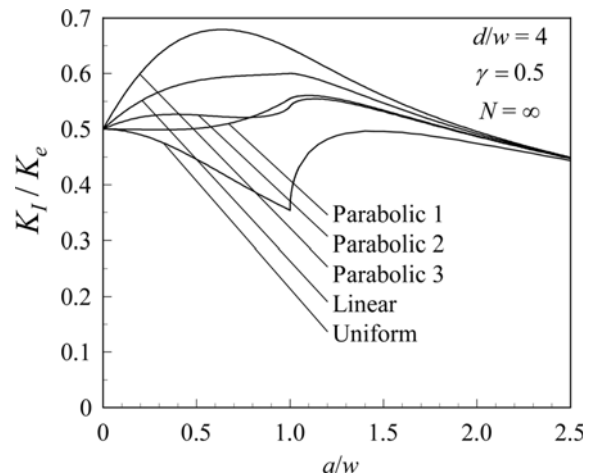


Fig. 7(b) Effect of eigenstrain distribution on the stress intensity factors ( $d/w = 4$ )

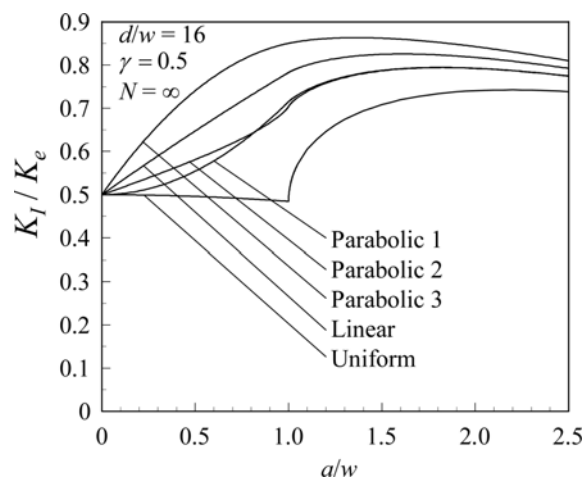


Fig. 7(c) Effect of eigenstrain distribution on the stress intensity factors ( $d/w = 16$ )

shown in Fig. 3. The results correspond to the crack spacing  $d/w = 0.5$ ,  $\gamma = 0.5$ ,  $N = \infty$ . The uniform distribution of eigenstrain is associated with the minimum stress intensity factor while the parabolic 3 distribution gives the maximum one. The average eigenstrain over the region of finite depth  $w$  is the maximum for the uniform distribution of eigenstrain among all the five distributions. This, in turn, induces the maximum magnitude of average compressive eigenstress. The compressive eigenstress has reducing effect on the resultant stress intensity factor. Therefore, the uniform distribution of eigenstrain gives the minimum stress intensity factor. On the other hand, the parabolic 3 distribution of eigenstrain has the minimum average value of eigenstrain over the region of finite depth  $w$ . This induces an average compressive eigenstress of the lowest magnitude attributing the least in the reduction of the resultant stress intensity factor. The other three curves of the stress intensity factor in Fig. 7(a) fall between the two curves corresponding to the uniform and parabolic 3 distributions of eigenstrain. This is due to the fact that the average values of these three distributions of eigenstrain fall between the average values of the uniform and parabolic 3 distributions of eigenstrain. Further, it is noted that, after certain value of the crack length ( $a/w > 1$ ), the stress intensity factor converges to the same value for all the distributions of the eigenstrain. Figs. 7(b) and 7(c) also exhibit the effect of the distribution of eigenstrain on the stress intensity factors, which are computed for the higher values of the crack spacing  $d/w$ . For the higher values of  $d/w$ , two features are observed. First, the point at which the stress intensity factors converge for all the distribution of eigenstrain moves to the right as the ratio  $d/w$  increases. Second, the concave shape of the curves of the stress intensity factors gradually turns to the convex shape as the ratio  $d/w$  increases. Therefore, it can be stated that, for higher value of crack spacing, most of the distributions of eigenstrain causes the stress intensity factor to increase with the increase of crack length within the finite region  $w$ .

Shown in Fig. 8(a) are the normalized stress intensity factors as a function of the parameter  $\gamma$  and normalized crack length  $a/w$ . The results correspond to  $d/w = 0.5$ ,  $N = \infty$ , and the linear

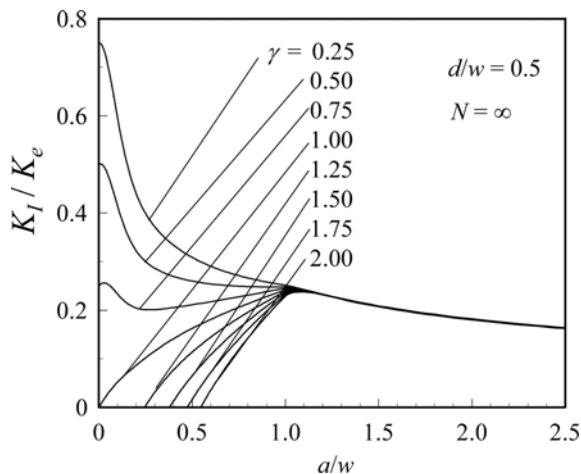


Fig. 8(a) Normalized stress intensity factors as a function of normalized crack length and the parameter  $\gamma$  for linear distribution of eigenstrain ( $d/w = 0.5$ )

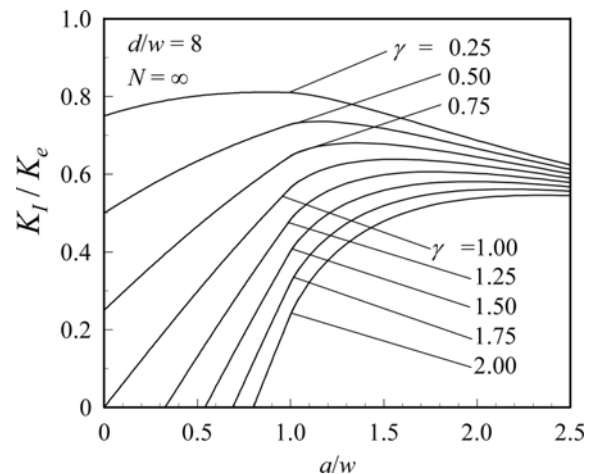


Fig. 8(b) Normalized stress intensity factor as a function of normalized crack length and the parameter  $\gamma$  for linear distribution of eigenstrain ( $d/w = 8$ )

distribution of eigenstrain. The higher value of  $\gamma$  indicates the higher magnitude of the eigenstrain at  $y = 0$ . This implies that the compressive eigenstress at  $y = 0$  has also a higher value. Thus, the stress intensity factor has a lower value when  $\gamma$  is higher, since the compressive eigenstress associated with the eigenstrain reduces the stress intensity factor. There is also another important point to be noted that when  $\gamma$  exceeds unity, crack closure occurs for a certain length of the crack, i.e., the crack surfaces are in contact and no stress intensity occurs. As an example, the stress intensity occurs only when  $a/w$  exceeds 0.4 for  $\gamma = 1.5$ . Fig. 8(b) shows the similar results corresponding to  $d/w = 8$ . Here, the curves of the stress intensity factors have the convex shape, which is opposite to that in Fig. 8(a).

In Fig. 9, normalized stress intensity factors are plotted as a function of normalized crack spacing  $d/w$  keeping the value of normalized crack length  $a/w$  constant ( $a/w = 0.5$ ). In the lower range of crack spacing, the stress intensity factor enhances as the distance  $d$  increases. After a certain value of  $d$ , the stress intensity factor becomes constant that indicates that one crack has no effect on the other, i.e., the single crack phenomenon is attained. This phenomenon has already been discussed with reference to Fig. 6.

The stress intensity factors as a function of normalized crack length and number of cracks are displayed in Fig. 10. The results correspond to the linear distribution of eigenstrain and  $d/w = 0.5$ ,  $\gamma = 0.5$ . The stress intensity factor is found to be decreased as the number of cracks increases. Fig. 11 portrays the stress intensity factors as a function of the normalized crack spacing and number of cracks for linear distribution of eigenstrain and  $a/w = 0.5$ ,  $\gamma = 0.5$ . In this case, it is also observed that the stress intensity factor decreases as the number of cracks increases. It is noted from the figure that, for higher value of crack spacing, the stress intensity factor becomes almost independent of crack number. This phenomenon is observed because the effect of one crack on the other diminishes as the crack spacing increases, and thus a single crack phenomenon is obtained.

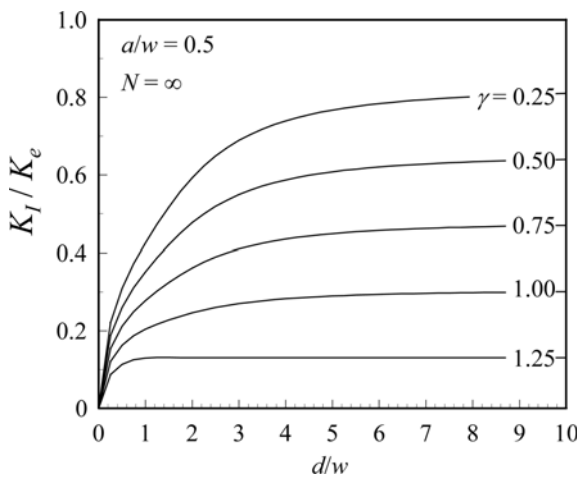


Fig. 9 Normalized stress intensity factor as a function of normalized crack spacing and the parameter  $\gamma$  for linear distribution of eigenstrain

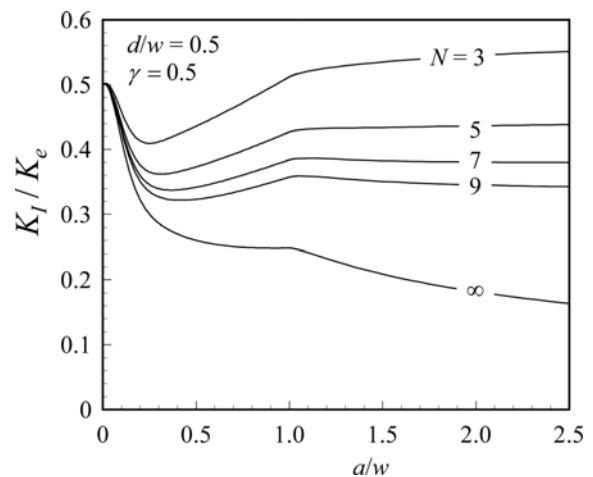


Fig. 10 Normalized stress intensity factor as a function of normalized crack length and the number of crack for linear distribution of eigenstrain

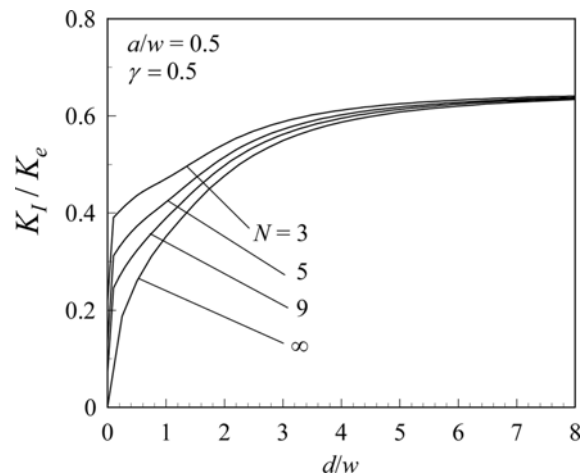


Fig. 11 Normalized stress intensity factor as a function of normalized crack spacing and the number of crack for linear distribution of eigenstrain

## 6. Conclusions

A simple as well as an effective method is developed to analyze stress intensity factors for a number of periodic edge cracks in a semi-infinite medium subjected to a far field uniform applied load along with an arbitrary distribution of eigenstrain. The method can be applied to calculate the stress intensity factors for a single edge crack by using a large value of the distance between the cracks. From the numerical results, it is noted that the stress intensity factors significantly depend on the distribution and the magnitude of the eigenstrain. The higher magnitude of average eigenstrain has higher effect on the stress intensity factors. The positive eigenstrain induces a compressive eigenstress that reduces the stress intensity factors. This reduction of the stress intensity factors is attributed to the toughening of the material. Further, the stress intensity factor also decreases as the number of cracks increases.

## Acknowledgements

The authors are grateful to Professor H. Sekine, Department of Aeronautics and Space Engineering, Tohoku University, Japan, for his useful and valuable suggestions and comments during the course of this work.

## References

- Afsar, A.M. (1997), "Analysis of edge cracks in semi-infinite functionally gradient materials with distributed eigenstrains", M.Sc. Dissertation, Tohoku University, Japan.
- Afsar, A.M. and Sekine, H. (2001), "Optimum material distributions for prescribed apparent fracture toughness in thick-walled FGM circular pipes", *Int. J. Pres. Vessels and Piping*, **78**, 471-484.

- Afsar, A.M. and Sekine, H. (2002), "Inverse problems of material distributions for prescribed apparent fracture toughness in FGM coatings around a circular hole in infinite elastic media", *Compos. Sci. Tech.*, **62**, 1063-1077.
- Benthem, J.B. and Koiter, W.T. (1973), "Asymptotic approximations to the crack problems", *Mechanics of Fracture-I, Methods of Analysis and Solutions of Crack Problems*, Edited by G.C. Sih, Noordhoff International Publishing, Leyden.
- Bowie, O.L. (1973), "Solutions of plane crack problems by mapping techniques", *Mechanics of Fracture-I, Methods of Analysis and Solutions of Crack Problems*, Edited by G.C. Sih, Noordhoff International Publishing, Leyden.
- Erdogan, F., Gupta, G.D. and Cook, T.S. (1973), "Numerical solution of singular integral equations", *Methods of Analysis and Solutions of Crack Problems* (G.C. Sih Ed.), Noordhoff International Publishing, Leyden 1.
- Hartranft, R.J. and Sih, G.C. (1973), "Alternating method applied to edge and surface crack problems", *Methods of Analysis and Solutions of Crack Problems 1* (G.C. Sih Ed.), Noordhoff International Publishing, Leyden.
- Hills, D.A., Kelly, P.A., Dai, D.N. and Korsunsky, A.M. (1996), "Distributed dislocation fundamentals", *Solution of Crack Problems-The Distributed Dislocation Technique* (Gladwell G.M.L. Ed.), Kluwer Academic Publishers.
- Krenk, S. (1975), "On the use of the interpolation polynomial for solution of singular integral equation", *Quart. Appl. Math.*, **32**, 479-484.
- Mura, T. (1987), *Micromechanics of Defects in Solids: Mechanics of Elastic and Inelastic Solids 3*, Kluwer Academic Publishers.
- Muskhelishvili, N.I. (1975), *Some Basic Problems of The Mathematical Theory of Elasticity (Translated from the Russian by J.R.M. Radok)*, Noordhoff International Publishers, The Netherlands.
- Sekine, H. and Afsar, A.M. (1999), "Composition profile for improving the brittle fracture characteristics in semi-infinite functionally graded materials", *JSME Int. J.*, Ser. A, **42**(4), 592-600.
- Sneddon, I.N. (1946), "The distribution of stress in the neighborhood of a crack in an elastic solid", *Proc. of The Royal Society of London*, **187A**, 229-260.
- Sneddon, I.N. and Das, S.C. (1971), "The stress intensity factor at the tip of an edge crack in an elastic half-plane", *Int. J. Eng. Sci.*, **9**, 25-36.
- Stallybrass, M.P. (1970), "A crack perpendicular to an elastic half-plane", *Int. J. Eng. Sci.*, **8**, 351-362.

## Notation

$\sigma_x^0$	: Applied stress
$\bar{\sigma}_x$	: Eigenstress
$\bar{\epsilon}_x$	: Eigenstrain
$a$	: Crack length
$d$	: Distance between the cracks
$w$	: Depth from free surface
$x-y$	: Principal coordinate system
$x_m-y_m$	: Secondary coordinate system
$z$	: Complex variable ( $= x + iy$ )
$s$	: Distance along the crack line
$E$	: Young's modulus
$\mu$	: Shear modulus
$\kappa$	: Kolosov's constant
$\nu$	: Poisson's ratio
$b_x, B_x$	: Dislocation density functions
$\Phi, \Psi$	: Complex potential functions
$t_q$	: Integration points
$\xi_r$	: Collocation points

$\gamma$  : Ratio of eigenstress to applied stress  
 $N$  : Number of cracks  
 $K_I$  : Stress intensity factor